Desalination and Water Treatment
www.deswater.com
doi: 10.5004/dwt.2018.22642

130 (2018) 63–70
October

Preparation of controlled porosity activated carbon from walnut shell for phenol adsorption

Abbas Akbarzadeh[a], Mohsen Arbabi[b,*], Sara Hemati[b,c]

[a]*Water Research Institute (WRI), The Institute for Energy and Hydro Technology (IEHT), Ministry of Energy, Tehran, Iran, email: abbasakbarzadeh@yahoo.com*
[b]*Departments of Environmental Health Engineering,School of Health, Social Determinants of Health Research Center, Shahrekord University of Medical Sciences, Shahrekord, Iran, Tel. +98 38 33333710; Fax:+98 38 33334678; email: m.arbabi @skums.ac.ir (M. Arbabi)*
[c]*Environmental Health Engineering, School of Health, Shahrekord University of Medical Sciences, Shahrekord, Iran, email: hemati.sara88@yahoo.com*

Received 2 October 2017; Accepted 18 June 2018

ABSTRACT

Phenol and its derivatives constitute widespread water pollutants. They have been found to accelerate tumor formation, cancer, and mutation. In this paper, walnut shell residue has been used as a raw material in preparation of powder activated carbon by the method of chemical activation with zinc chloride for the adsorption of phenol from dilute aqueous solutions. The influence of the mass impregnation ratio (R = $ZnCl_2$/walnut shell) and physical activation by the CO_2 stream on the physical and chemical properties of the prepared carbons was examined. The effects of main parameters such as contact time (t), initial phenol concentration (C_o), and solution's pH were studied on phenol adsorption. The maximum uptake of phenol at 25°C was 214 mg g^{-1} at pH near phenol pK_a and C_o = 1,000 mg L^{-1}. All data were fitted well with Langmuir isotherm, but after CO_2 modification, deviation from Langmuir shows that both physical and chemical adsorption occurred during adsorption. The kinetic data were fitted to different models such as pseudo-first-order, pseudo-second-order, and diffusion model. Pseudo-second-order model has been chosen as the best model. In overall, walnut shell shows excellent adaptive characteristics for the removal of phenol and appears as a very promising sorbent due to its high uptake capacity and to its low cost.

Keywords: Adsorption; Activated carbon; Walnut shell; Phenol

1. Introduction

Activated carbon in its broadest sense includes a wide range of processed amorphous carbon-based materials with a large internal surface area and pore volume, which are usually rich in oxygen and hydrogen. These heteroatoms are derived from the starting material and become a part of the chemical structure, as a result of imperfect carbonization, either they become chemically bonded to the surface during activation or during subsequent treatments; therefore, many functional groups on activated carbon have oxygen atom. The functional groups on activated carbon can be increased by treating it with some oxidizing agents or decreased by exposing it to a vacuum environment at very high temperature [1]. In general, the carbonaceous surface can be regarded as consisting of the carbon basal planes and various functional groups [2].

Phenol and its derivatives constitute widespread water pollutants. They have been found to accelerate tumor formation, cancer, and mutation [3]. These compounds are usually found in the wastewaters from industrial effluents such as plastic, coal, tar, gasoline, disinfectant, pharmaceutical, and agro-industrial processes such as the olive oil mills, tomato processing, and wine distillers [4].

* Corresponding author.

The various treatment techniques available for removal of phenol from fluid stream are ion exchange, evaporation, reverse osmosis, reduction, chemical precipitation, membrane, adsorption, etc. Most of these methods suffer from drawbacks such as high capital and operational costs [5].

Adsorption is one of the most effective processes of advanced wastewater treatment. It requires low capital cost; furthermore, there are abundant low-cost available materials which can be used as adsorbents [6]. Activated carbon is the most important material which is used as an adsorbent to clean environmental pollution such as gases and liquid impurities [7]. It has a large adsorption capacity for a variety of organic pollutants but it is expensive due to its difficult regeneration and higher disposal cost [8].

The activated carbon adsorption capacity depends on quite different factors. Obviously, it depends on the different characteristics of activated carbon such as texture (surface area and pore size distributions), surface chemistry (surface functional groups), and ash content. The qualities and characteristics of activated carbon depend on the physical and chemical properties of the precursor materials and activation methods [7]. In this field, the main goals of different studies were increasing adsorption capacity [9], pore size distribution optimization [10], utilizing low-cost raw materials [11–17], and modification of adsorbents characteristics [18–20].

Recently, in spite of many literatures that has worked on using waste material for preparation of activated carbon, is still a challenge to prepare activated carbon with very specific characteristics, such as a given pore size distribution, and using low-cost raw materials processed at low temperature (less energy costs) [21]. Besides, it shows that although many activated carbons were made by $ZnCl_2$ activated agent in previous researches, but there are scarce studies that investigate the effect of gas modification on adsorption [22–24]. Furthermore, it has been shown that the differences in adsorption uptakes were mainly as a result of the differences in their functional groups which are formed during modification [25].

In this paper, we produced activated carbons with promising pore size distribution for improving phenol adsorption capacity by using walnut shell as a low-cost precursor and zinc chloride as an activated agent. Then prepared adsorbents (sample is coded *R*) were modified by CO_2 gasification (sample is coded RC) to study the effect of CO_2 modification on adsorption of phenol from aqueous solution. Also, the effect of various parameters such as solution pH, activated carbon functional groups, and diffusion rate was examined on phenol adsorption.

2. Experimental techniques

2.1. Preparation of activated carbon

The walnut shells used for the preparation of nanoporous adsorbent were prepared from agriculture waste industry. It was reduced to the size of 2–3.5 mm with a hammer mill. The sized shell was washed with distillate water to remove the surface adhered particles and water-soluble impurities. The filtered materials were dried in 80°C at the oven overnight to eliminate moisture. At the first step of activation, the starting material was mixed into a boiling solution containing zinc chloride with weight ratios of 0.75, 0.82, and 1 to walnut shell (samples are coded R = 0.75, R = 0.82, and R = 1). The mixture was then dried at 110°C to prepare the impregnated sample. In all experiments, heating rate, activation temperature, and nitrogen flow rate were kept constant.

In the second step, the resulting chemical loaded sample was placed on a quartz, which was then inserted in a quartz tube (id = 25 mm). The impregnated sample was heated up to activation temperature 450°C under N_2 flow (300 mL min^{-1}) at the rate of 5°C min^{-1} and held at the activation temperature for 55 min. Activated sample was cooled down under N_2 flow and washed with 0.5 N HCl, hot water and finally cold distilled water to remove residual organic and mineral until it did not give a Cl reaction with $AgNO_3$. Then washed sample was dried at 110°C to prepare activated carbon. For physical activation prepared activated carbon was heated up to 900°C under 5% CO_2 in N_2 stream at the rate of 5°C min^{-1} and held at the activation temperature for 5 h (samples are coded RC = 0. 75, RC = 0. 82, RC = 1). The resulting activated carbon was characterized by using an accelerated surface area and porosimetry system (ASAP 2010, Micromeritics) under N_2 adsorption at 77 K using the Brunauer–Emmett–Teller (BET) equation [26–28]. The micropore volume and the nonmicropore surface area were calculated by using the *t*-plot method using a standard adsorption isotherm for activated carbons [29]. The total pore volume was estimated to be the liquid volume of adsorbates (N_2) at a relative pressure of 0.985.

2.2. Infrared spectroscopy

A quantitative analysis of activated carbon was conducted by obtaining Fourier-transform infrared spectroscopy (FTIR) transmission spectra of carbon samples by KBr technique [30]. The technique was conducted by placing the KBr powder, ground with an agate mortar in the sample cup and then the powder surface was evened by using the attached sample pressing bar. Next, the powder was mounted to the instrument to make a background measurement. After that, the activated carbon sample was diluted with the KBr powder with the ratio of 10% and grounded with the agate mortar until it became fine particles to mix the both kinds. Then, the mixed powder was placed in the sample cup and the powder surface was also evened by using the sample pressing bar. Finally, the mixed powder was mounted to the instrument to make a sample measurement in the transmittance %T mode. The analysis was carried out by Shimadzu 8400S FTIR instrument in the wave number range of 400–500 cm^{-1}.

2.3. Phenol adsorption procedure

The study of phenol adsorption took place in a constant temperature bath (25°C) under continuous shaking. Ultrapure phenol was obtained from Merck (KIMIA NOAVAR AZMA Company, Tehran, Iran). A stock phenol solution was prepared initially at concentration of 50 g L^{-1}, using distillated and deionized water. Adsorption kinetics and equilibrium studies were conducted by using the bottle point isotherm technique and placing a known quantity of the adsorbent (0.1 g) in glass bottle containing 50 mL of an aqueous solution of phenol at various concentrations (0–1,000 mg L^{-1}). After solution preparation, each bottle was shaken in a thermostatic incubator shaker for specific time intervals till the equilibrium was reached. The kinetic experiments were carried out by two different concentrations, namely 500 and 1,000 ppm.

Sodium hydrogen phosphate (analytical grade, obtained from Merck) was also added at concentration of 10^{-3} M in order to provide sufficient buffer capacity during phenol adsorption. The contaminated aqueous solution pH was fixed at desire pH. After the equilibration period, the carbons were filtered and analyzed for phenol concentration following the direct photometric method. In this method, the phenol concentration in the wastewater was monitored using a UV–visible spectrophotometer (WTW, Germany) working at 500 nm. All measurements performed in duplicate and experimental errors were found below 8%. The quantity of phenol capacity (q_t) calculated the difference between the initial (C_o) and the instant concentrations (C_t), $q_t = (C - C_tV/m)$ (m and V are adsorbent mass and the volume of the contaminated solutions, respectively).

3. Result

3.1. Effect of chemical impregnation ratio (R) and modification on adsorption capacity

The effect of chemical impregnation ratio ($ZnCl_2$ to nutshell ratio) on BET surface area, micropore volume and total pore volume of activated carbons are shown in Figs. 1 and 2, respectively. For all these samples the carbonization temperature and time were 450°C and 55 min, respectively. The effect of oxidation on BET surface areas varies according to the treatment used and the raw material properties (Table 1). Fig. 2 represents the effect of the chemical ratio in terms of adsorption capacity for better prepared and modified samples. For better examination, the results comprised with a commercial adsorbent means NORIT 830W for wastewater treatment (see Fig. 3).

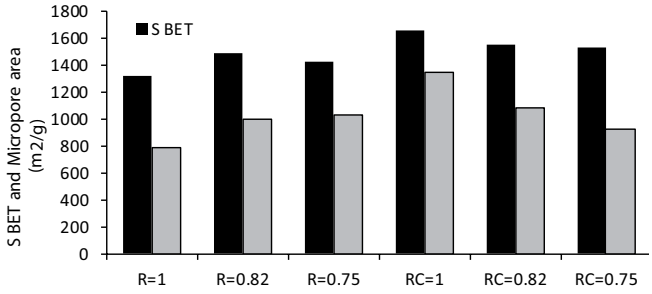

Fig. 1. Effect of impregnation ratio on S_{BET} and microporous area.

3.2. Effect of CO_2 modification on carbon functional group

The FTIR measurements were performed in order to confirm the formations of functional groups upon oxidation. Fig. 4 shows the FTIR of our best sample before and after modification. The FTIR spectrums for all adsorbents revealed that there were various functional groups detected on the prepared activated carbon. All spectra treatment shows a wide absorption band at 3,200–3,600 cm^{-1} maximum at about 3,420–3,440 cm^{-1}. The board band at this adsorption band 1,715 cm^{-1} can be related to delegate to O–H stretching vibration of hydroxyl functional groups and adsorbed water. Other peaks detected on the activated carbons were justified to aliphatic with the adsorption band between 2,910 and 2,850 cm^{-1} containing C–H stretching in $–CH_2–$; and at

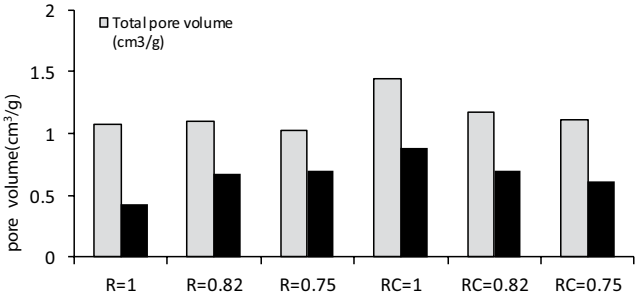

Fig. 2. Effect of impregnation on total and micropore volumes.

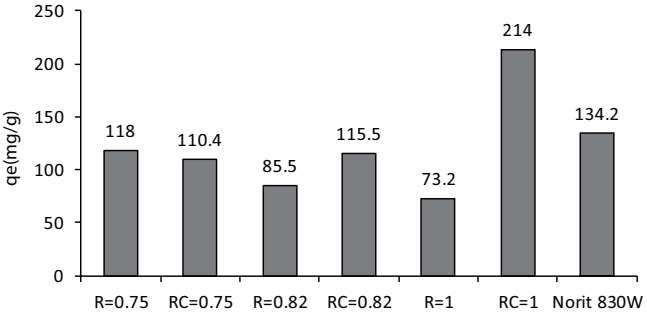

Fig. 3. Effect of impregnation on adsorption capacity and comparison with Norit 830W at pH = 7.1.

Table 1
N_2 adsorption data of prepared and modified adsorbent

Properties	R = 1	R = 0.82	R = 0.75	RC = 1	RC = 0.82	RC = 0.75
BET surface area[a] ($m^2\ g^{-1}$)	1,325.1	1,496.3	1,430.9	1,655.5	1,551.4	1,532.9
Micropore area ($m^2\ g^{-1}$)	785.8	995.6	1,034.1	1,353.4	1,086.7	923.3
Total pore volume[b] ($cm^3\ g^{-1}$)	1.07	1.01	1.03	1.45	1.18	1.11
Micropore volume ($cm^3\ g^{-1}$)	0.432	0.671	0.703	0.883	0.696	0.613
Average pore diameter (Å)[c]	14.22	13.36	11.13	18.16	15.54	13.14
Fractional microporosity (%)[d]	40	61	68	62	58	55

[a]P/P_o range from 0 to 0.22.
[b]Single point desorption total pore volume of pores less than 3,000 Å at P/P_o = 0.985.
[c]Applying BET mode.
[d]Micropore volume/total pore volume × 100%.

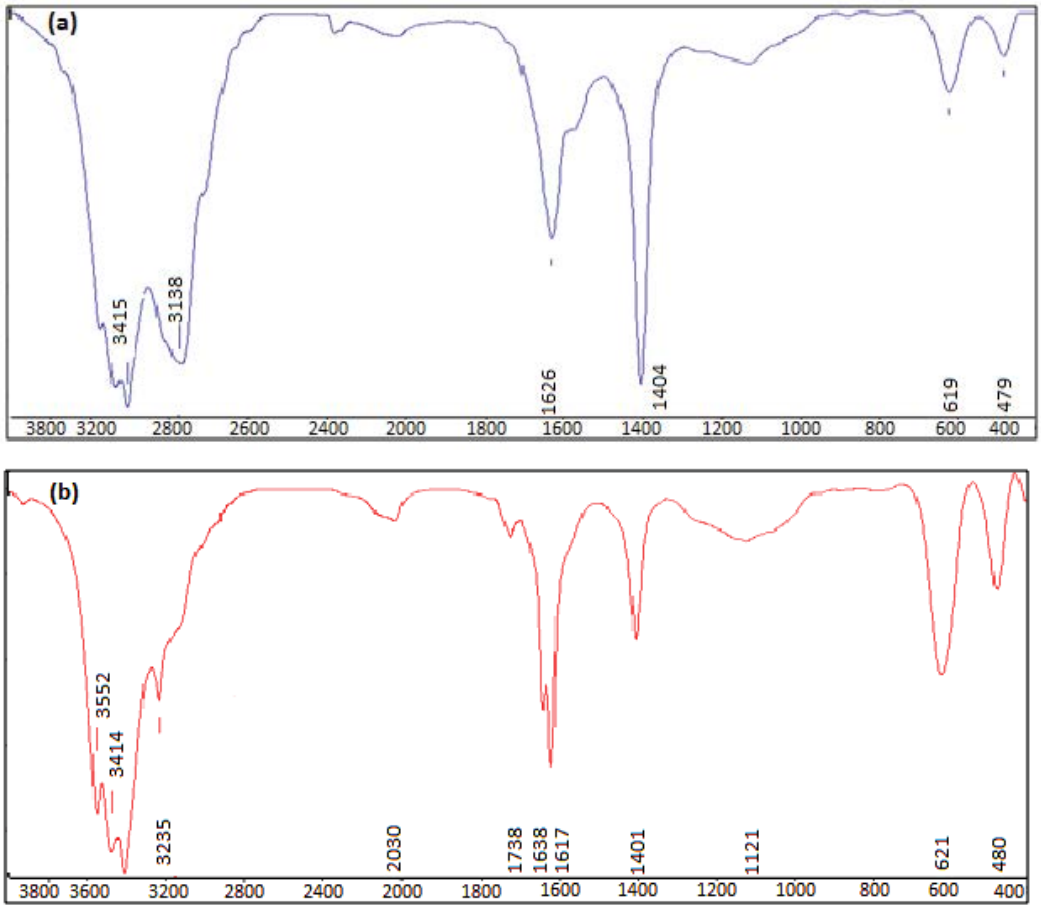

Fig. 4. FTIR of samples (a) R = 0.75 and (*b*) RC = 1.

1,401 cm^{-1} related to $–CH_2–$ deformation and aromatic structures. A very small peak at 1,720 cm^{-1} is usually assigned to C=O stretching vibrations of aldehydes, ketones, lactones, or carboxyl groups. The FTIR spectra also show a strong band at 1,638–1,600 cm^{-1} due to aromatic ring stretching vibration (C=C) enhanced by polar functional groups. The wide bands at 1,300–1,000 cm^{-1} have been assigned to C–O stretching in acids, alcohols, phenols, ether, and esters. A small peak at 1,715 cm^{-1} changed to the large peak because CO_2 modification partially oxides functional groups by creating a hydroxyl functional group.

3.3. Effect of pH on adsorption capacity

Solution pH is one of the key factors that control the adsorption process of organic weak electrolytes because it controls the electrostatic interactions between the adsorbent and the adsorbate.

Phenol has a pK_a value of 9.95; therefore, below this value of pH, this compound will be found in solution predominantly in the molecular form. Above it, the ionic form is predominant. Because the hydroxyl group is an activating group, the ring is partially negatively charged. Figs. 5 and 6 represent the effect of pH on the adsorption capacity of prepared and modified activated carbon. It is clear that at lowest and highest pH, adsorption capacity is minimum.

3.4. Adsorption isotherms

In this study, the sorption capacity and equilibrium isotherm for phenol onto activated carbon are estimated. The experimental data are interpreted by Langmuir, Freundlich, and Toth isotherms. In Fig. 7 the comparison between adsorption isotherm of phenol for R = 1 is presented.

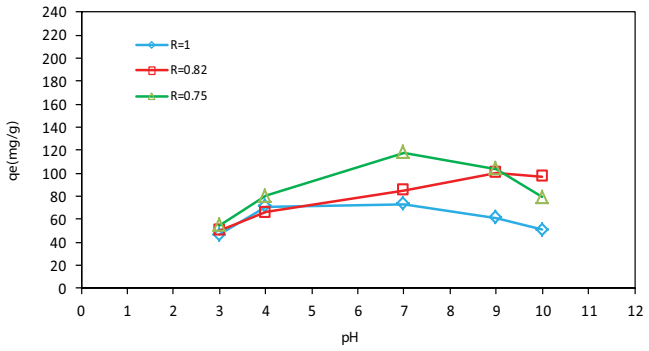

Fig. 5. Effect of pH on phenol removals. Conditions: prepared activated carbon, adsorbent dose 2 g L^{-1}, initial concentration of phenol 1,000 mg L^{-1}, agitation time 72 h, agitation speed 140 rpm, and temperature 25°C.

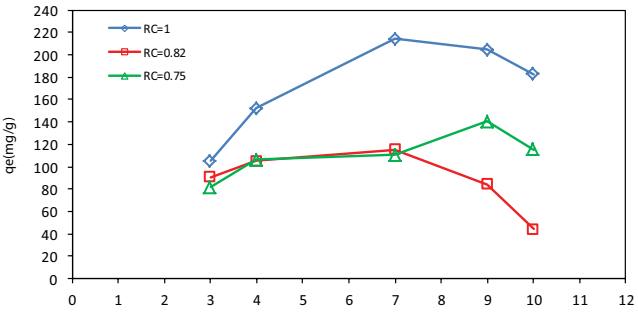

Fig. 6. Effect of pH on phenol removals. Conditions: modified activated carbon, adsorbent dose 2 g L^{-1}, initial concentration of phenol 1,000 mg L^{-1}, agitation time 72 h, agitation speed 140 rpm, and temperature 25°C.

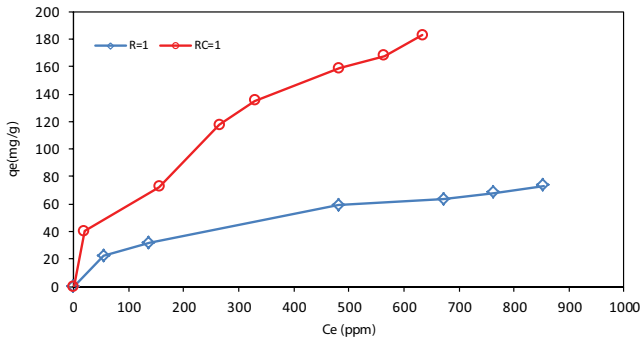

Fig. 7. Adsorption isotherms of phenol onto the prepared R = 1 and modified activated carbon RC 1 at pH = 7, stirring = 140 rpm, and temperature = 25°C.

3.5. Kinetics model

3.5.1. Pseudo-first-order kinetic model

The adsorption kinetic data of phenol are analyzed by using the Lagergren first-order rate equation. This model based on solid capacity is normally expressed as follows [31]:

$$\log\left(q_e - q\right) = \frac{\log q_e - k_1 t}{2.303} \tag{1}$$

where q_e and q are the amount of phenol adsorbed (mg g^{-1}) at equilibrium and at time t (h), respectively, and k_1 is the Lagergren rate constant of pseudo-first-order adsorption (L min^{-1}). Value of k_1 calculated from the slope of the plot of $\log(q_e - q)$ versus t is shown in Table 2. It was found that the calculated q_e values do not agree with the experimental q_e values. This suggests that the adsorption of phenol on prepared activated carbon does not follow pseudo-first-order kinetics model (see Table 2).

3.5.2. Pseudo-second-order model

The pseudo-second-order kinetics model additionally based on solid capacity can be represented as follows:

$$\frac{t}{q} = \frac{1}{k_2 q_e^2} + \frac{t}{q_e} \tag{2}$$

where k_2 is the equilibrium rate constant of pseudo-second-order adsorption (min g mg^{-1}) [32]. The relevance of this model can be examined by linear plot of (t/q) versus t, presented in Figs. 8 and 9. In order to quantify the applicability of model, the correlation coefficient (R^2) was calculated from this plot. Value of equation parameters is shown in Table 2. The calculated q_e values agree with experimental q_e values and also the correlation coefficients for the second-order kinetic plots at all the studied concentrations were above 0.99.

3.6. Diffusion model

The intraparticle diffusion model is based on the theory proposed by Weber and Morris. According to this theory

$$q = k_d \sqrt{t} + \theta \tag{3}$$

where k_d (mg g^{-1} $h^{1/2}$) is the intraparticle diffusion rate constant (mg g^{-1} $min^{-1/2}$), and θ (mg g^{-1}) is a constant related to the thickness of the boundary layer (see Table 3). The layer is the value of θ, the greater is the boundary layer effect. If the so-called Weber–Morris plot of q_t versus $t^{1/2}$ gives a straight line, then the sorption process is controlled by intraparticle diffusion only. However, if the data exhibit multilinear plots, then two or more steps influence the sorption process. The first sharper portion is the external surface adsorption or instantaneous adsorption stage. The second portion is the gradual adsorption stage, where the intraparticle diffusion is rate limited. The diffusion model plots shown in Fig. 10 suggest two-stage adsorption process, surface adsorption and

Table 2
Determined kinetic model constants for the adsorption of phenol on different activated carbon (pH = 7, C_0 = 1,000 mg L^{-1}, T = 25°C)

Adsorbent	Pseudo-first-order		Pseudo-second-order			
	k_{1e} (h^{-1})	R^2	k_2 (g mg^{-1} h^{-1})	R^2	q_e (mg g^{-1})	
					Experimental	Calculated
R = 1	0.5142	0.89	0.034	0.99	73.2	73.16
R = 0.82	0.4387	0.93	0.026	0.99	85.5	88.26
R = 0.75	0.3601	0.87	0.019	0.99	118.00	118.70
RC = 1	0.4242	0.94	0.043	0.99	214.3	212.02
RC = 0.82	0.3274	0.97	0.013	0.99	115.5	116.03
RC = 0.75	0.2839	0.82	0.020	0.99	110.4	111.09

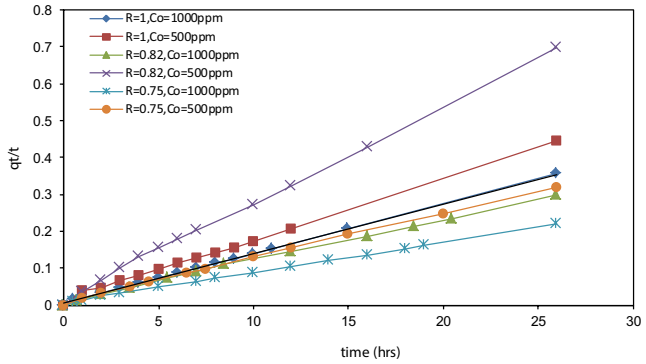

Fig. 8. Pseudo-second-order model plot for phenol adsorption on prepared activated carbon at pH = 7, T = 25°C.

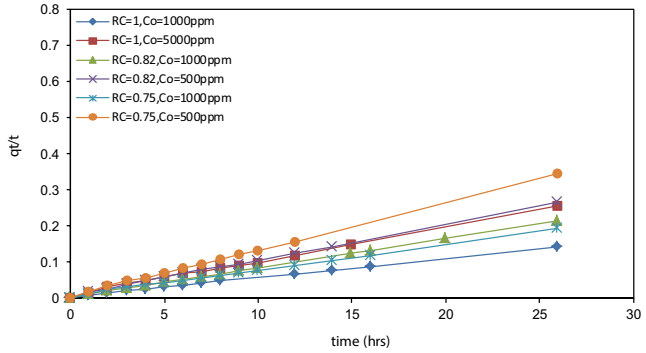

Fig. 9. Pseudo- second- order model plot for phenol adsorption on modified activated carbon at pH = 7, T = 25°C.

Table 3
Intraparticle diffusion rate constants (k_d and θ) at C_0 = 1,000 mg L^{-1}, pH = 7, T = 25°C

Adsorbent	Intraparticle diffusion rate		
	k_d (mg $g^{-1}.h^{0.5}$)	θ	R^2
R = 1	7.07	59.36	0.94
R = 0.82	5.40	63.37	0.95
R = 0.75	9.30	89.62	0.96
RC = 1	14.08	125.8	0.96
RC = 0.82	12.07	83.13	0.96
RC = 0.75	26.76	51.87	0.96

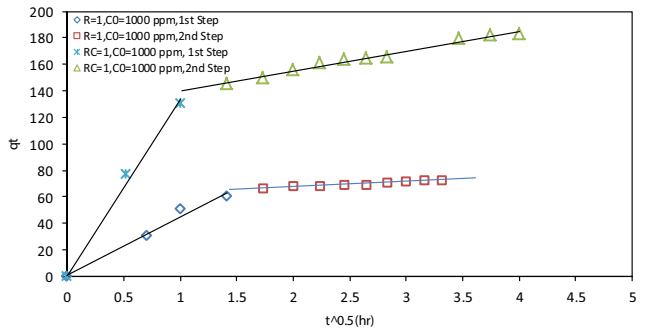

Fig. 10. Intraparticle diffusion model plot for phenol adsorption on R = 1 and RC = 1 samples.

intraparticle diffusion. The first linear portion of the plots indicates boundary layer effect, that is, surface adsorption, while the second linear portion is due to the intraparticle/pore diffusion within the pores of activated carbons.

4. Discussion

According to Fig. 1 shown in Section 3, surface area as well as the total pore volume increases with an increase in chemical impregnation ratio. It was observed that an excess amount of $ZnCl_2$ significantly enhances the process of pore widening and formation of the micro- and mesoporous structure by promoting externally located devolatilization process. Also, it can be seen that porosity evolution is different before and after modifying by CO_2 stream.

Reaction of oxygen molecules on CO_2 with carbon in an activated carbon surface area intensifies micropore area and volume by oxygen chemisorptions on the pore walls (volume reduction) and oxidation of the carbon material (widening and/or formation of new pores). As a result of developing micropore volume, the surface area increases in all samples by reforming with CO_2 molecules (Table 1).

As depicted in Figs. 2 and 3 shown in Section 3, in prepared samples, an increase in pore size distribution causes that the effect of interaction between phenol molecules and the basal plan in the carbon structure decreases and low adsorption capacity is obtained. In modified samples appropriate pore size distribution for phenol adsorption and formation of COOH functional groups lead to increase in adsorption capacity of phenol molecules.

Adsorption of phenol by activated carbon is divided into physisorption and chemisorptions. Physisorption of phenolic compounds to carbon surfaces is thought to arise from dispersion forces acting between π-electrons in the graphite basal planes on the surface. Physisorption is reduced as a result of π-electron localization and is increased when electron withdrawing substituent groups on the phenol molecule decrease the electron density of the ring [33]. Finally, chemisorptions may occur between phenol and specific sites on the surface, and could be partly responsible for irreversible adsorption. In adsorption of phenolic compounds from aqueous solution irreversible chemisorptions could occur on oxygen-free sites located at the edges of the graphene layers, whereas others have proposed that phenolic groups and oxygen-containing basic groups can promote irreversible adsorption [34]. Also phenol molecules or phenoxy radicals react with active sites on a carbon surface, which can result in covalent bonding to the surface.

The results show that at solution pH near pK_a, its uptake increased because the surface charged would be on average positively charged and screened by the increase in the electrolyte concentration, resulting in an enhancement of the phenol uptake. The highest adsorption of phenols occurred at pH 6.5 and 9.0 for all adsorbents. Reduction in adsorption at pH 9 is possibly due to the increased solubility of phenol, the abundance of OH ions thereby increasing hindrance to diffusion of phenol ions and also increases electrostatic repulsion between the negatively charged surface sites of the sorbent and phenolic ions.

For acidic pH, phenol is in the molecular form and only the dispersive interactions are expected to play an important

role in its adsorption on the carbon surface. In modified samples, they have the highest amount of oxygen-containing surface groups and consequently the lowest electronic density in the basal planes, which should lead to weaker dispersive interactions. In addition, there is competition between water and phenol molecules. Water can form hydrogen bonds with the hydrophilic groups on the carbon surface originating clusters that may obstacle the passage of molecules to micropore. Also creating oxygen-containing surface groups by modifying with CO_2 stream has this effect on adsorption by (1) obstructing the pass and (2) producing repulsion force to weak electrolytes.

At basic pH, because phenol is almost completely in the anionic form, the maximum adsorption capacity (q_m) is not significantly affected. It can be due to bonds between water and anions, which are stronger and more difficult to break before the adsorption. Another reason is that because at this pH phenol is almost completely in the anionic form and in these conditions all carbon samples are negatively charged; therefore, an electrostatic repulsion phenomenon is produced.

All of the isotherms model parameters have been reported in Table 4. According to Table 4, the correlation coefficients (r^2) showed the fit between experimental data and isotherm equations, while the average percentage errors (D%) according to below equation indicated the fit between the experimental and predicted values of adsorption capacity. Where, N is the number of experimental data [13]. As seen from Table 4, Freundlich and Langmuir equation represent poorer fit of experimental data than the Toth isotherm equation. The Toth isotherm generates a satisfactory fit to the experimental data as indicated by correlation coefficients and average percentage error. The average percentage error values lie between 0.96% and 4.32%. This is the best general equation for describing most of the organic-aqueous equilibrium systems. It can be seen that only for sample R = 0.82 the Freundlich isotherm fits its data by lower average percentage error in comparison with other equations:

$$\left(D\%\right)=\left(1/N\right)\sum[q_e^{\exp}-q_e^{\mathrm{pre}}]/q^{\exp}\times 100 \quad (4)$$

The equilibrium data fit perfectly the Toth model of sorption, show the heterogeneous distribution of active sites on the activated carbon surface. The use of Toth isotherm suggests a heterogeneous adsorption process, typified by a Freundlich equation, but there is a tendency to form a monolayer saturation capacity, typical of the classical Langmuir equation [35].

The results indicated that the pseudo-second-order model describes the sorption kinetics of the system studied more appropriately than the pseudo-first-order model.

5. Conclusion

Activated carbons have been prepared from walnut shells by chemical activation with $ZnCl_2$. The optimal condition for preparing microporous activated carbon with high pore surface area and pore volume is an impregnation ratio of 100% (ratio of $ZnCl_2$ to walnut shells). The best performances were obtained for modified activated carbon that combines a high surface area and total pore volume. At this optimal condition, the BET surface area and total pore volume are 1,655.5 $m^2\ g^{-1}$ and 1.45 $cm^3\ g^{-1}$, respectively. Too large ratio of $ZnCl_2$ to walnut shells residue produces pore widening resulting in a mesoporous carbon pore structure. Batch studies show that a simple model of pseudo-second-order kinetic equation can adequately predict the adsorption of phenol on the apatite surface. The adsorption capacity is strongly dependent on the aqueous phase pH. Further analyses suggest that the sorption process is controlled by intraparticle diffusion of phenol. The results show that CO_2 modification increases the physical adsorption by forming COOH functional group at activated carbon porous, which it changes the adsorption isotherm to pseudo-first and pseudo-second-order which used to fit Langmuir isotherm before modification. Furthermore, CO_2 modification evaluates the adsorbent pore size distribution which it increases in pore structure heterogeneity. As a brief result, in optimum condition (C_0 = 1,000 mg L^{-1}, t = 25°C) the adsorption ratio was 214 mg g^{-1}. In overall, walnut shell shows excellent adsorptive characteristics for the removal of phenol and appears as a very promising sorbent due to its high uptake capacity and to its low cost.

References

[1] R.C. Bansal, M. Goyal, Activated Carbon Adsorption, CRC Press, Boca Raton, 2005.
[2] M. Arbabi, S. Hemati, S. Raygan, M. Sedehi, A. Khodabakhshi, A. Fadaei, Evaluation of almond shells magnetized by iron

Table 4
Isotherm constant of the Langmuir, Freundlich, and Toth models for phenol adsorption by activated carbons (pH = 7, C_0 = 1,000 mg L^{-1}, T = 25°C)

Adsorbent	Langmuir isotherm				Freundlich isotherm				Toth isotherm				
	q_{mon} (mg g^{-1})	k_L(L g^{-1}) × 1,000	R^2	D%	k_F	N	R^2	D%	a	b	n	R^2	D%
R = 1	87.56	4.73	0.98	1.85	3.81	2.29	0.99	1.2	3,146.4	1.65	0.135	0.99	1.26
R = 0.82	87.64	3.48	0.73	13.25	2.61	2.05	0.97	2.81	900,925.1	1.39	0.06	0.85	4.32
R = 0.75	124.84	6.72	0.94	6.51	9.91	2.77	0.91	2.21	5,981.7	0.97	0.1	0.96	2.01
RC = 1	233.8	4.47	0.89	3.32	6.11	1.89	0.97	1.6	51,743.2	2.21	0.12	0.99	1.02
RC = 0.82	144.32	4.77	0.97	2.96	8.15	2.48	0.89	2.13	111.8	779611	2.47	0.99	0.96
RC = 0.75	134.31	4.63	0.97	5.32	3.32	1.89	0.98	1.26	456	3.789	0.3	0.99	1.41

$D\% = (1/N)\sum|q_e^{\exp} - q_e^{\mathrm{pred}}|/q_e^{\exp} \times 100$. N is the number of experimental data.

nano-particles for nitrate removal from aqueous solution: study of adsorption isotherm, J. Shahrekord Univ. Med. Sci., 17 (2016) 92–102.
[3] C. Namasivayam, D. Sangeetha, Recycling of agricultural solid waste, coir pith: removal of anions, heavy metals, organics and dyes from water by adsorption onto $ZnCl_2$ activated coir pith carbon, J. Hazard. Mater., 135 (2006) 449–452.
[4] K.P. Singh, A. Malik, S. Sinha, P. Ojha, Liquid-phase adsorption of phenols using activated carbons derived from agricultural waste material, J. Hazard. Mater., 150 (2008) 626–641.
[5] S. Berardinelli, C. Resini, L. Arrighi, Technologies for the removal of phenol from fluid streams: a short review of recent developments, J. Hazard. Mater., 160 (2008) 265–288.
[6] K. Mohanty, D. Das, M. Biswas, Adsorption of phenol from aqueous solutions using activated carbons prepared from *Tectona grandis* sawdust by $ZnCl_2$ activation, Chem. Eng. J., 115 (2005) 121–131.
[7] Y. Önal, B.C. Akmil, O. Sarici, S. Erdogan, Textural development of sugar beet bagasse activated with $ZnCl_2$, J. Hazard. Mater., 142 (2007) 138–143.
[8] M.C. Burleigh, M.A. Markowitz, M.S. Spector, B.P. Gaber, Porous polysilsesquioxanes for the adsorption of phenols, Environ. Sci. Technol., 36 (2002) 2515–2518.
[9] M.C. Xu, Y. Zhou, J.-H. Huang, Adsorption behaviors of three polymeric adsorbents with amide groups for phenol in aqueous solution, J. Colloid Interface Sci., 327 (2008) 9–14.
[10] S. Hacein-Bey-Abina, C. Von Kalle, M. Schmidt, F. LeDeist, A serious adverse event after successful gene therapy for X-linked severe combined immunodeficiency, N. Eng. J. Med., 348 (2003) 255–256.
[11] J.M. Dias, M.C. Almeida, J. Rivera, M. Sanchez Polo, Waste materials for activated carbon preparation and its use in aqueous-phase treatment: a review, J. Environ. Manage., 85 (2007) 833–846.
[12] A. Puziy, O. Poddubnaya, A. Martinez, F. Suarez, J.M.D. Tascon, Synthetic carbons activated with phosphoric acid: I. Surface chemistry and ion binding properties, Carbon, 40 (2002) 1493–1505.
[13] B. Hameed, A. Rahman, Removal of phenol from aqueous solutions by adsorption onto activated carbon prepared from biomass material, J. Hazard. Mater., 160 (2008) 576–581.
[14] A.T. Din, B. Hameed, A.L. Ahmad, Batch adsorption of phenol onto physiochemical-activated coconut shell, J. Hazard. Mater., 161 (2009) 1522–1529.
[15] P. Girods, A. Dufour, V. Fierro, Y. Rogaume, C. Rogaume, A. Zoulalian, A. Celzard, Activated carbons prepared from wood particleboard wastes: characterisation and phenol adsorption capacities, J. Hazard. Mater., 166 (2009) 491–501.
[16] S.H. Lin, R.S. Juang, Adsorption of phenol and its derivatives from water using synthetic resins and low-cost natural adsorbents: a review, J. Environ. Manage., 90 (2009) 1336–1349.
[17] M. Ahmaruzzaman, Adsorption of phenolic compounds on low-cost adsorbents: a review, Adv. Colloid Interface Sci., 143 (2008) 48–67.
[18] G. Stavropoulos, P. Samaras, G. Sakellaropoulos, Effect of activated carbons modification on porosity, surface structure and phenol adsorption, J. Hazard. Mater., 151 (2008) 414–421.
[19] R. Berenguer, J.P. Marco Lozar, D. Cazorla Amoros, E. Morallon, Effect of electrochemical treatments on the surface chemistry of activated carbon, Carbon, 47 (2009) 1018–1027.
[20] G. Liu, J. Ma, X. Li, Q. Qin, Adsorption of bisphenol A from aqueous solution onto activated carbons with different modification treatments, J. Hazard. Mater., 164 (2009) 1275–1280.
[21] Y. Sudaryanto, S.B. Hartono, W. Irawaty, H. Hindarso, S. Ismadji, High surface area activated carbon prepared from cassava peel by chemical activation, Bioresour. Technol., 97 (2006) 734–739.
[22] M.J. Prauchner, F. Rodriguez-Reinoso, Preparation of granular activated carbons for adsorption of natural gas, Microporous Mesoporous Mater., 109 (2008) 581–584.
[23] M.K.B. Gratuito, T. Panyathanmaporn, R.A. Chumnanklang, A. Dutta, Production of activated carbon from coconut shell: optimization using response surface methodology, Bioresour. Technol., 99 (2008) 4887–4895.
[24] Y. Nakagawa, M. Molina-Sabio, F. Rodríguez-Reinoso, Modification of the porous structure along the preparation of activated carbon monoliths with H_3PO_4 and $ZnCl_2$, Microporous Mesoporous Mater., 103 (2007) 29–34.
[25] F. Rodriguez-Reinoso, J.M. Martin-Martinez, C. Prado-Burguete, B. Mcenaney, A standard adsorption isotherm for the characterization of activated carbons, J. Phys. Chem., 91 (1987) 515–516.
[26] T. Budinova, E. Ekinci, A. Grimm, E. Bjornbom, V. Minkova, M. Goranova, Characterization and application of activated carbon produced by H_3PO_4 and water vapor activation, Fuel Process. Technol., 87 (2006) 899–905.
[27] S. Carabineiro, T. Thvorn, M.F.R. Pereira, J.L. Figueiredo, Adsorption of ciprofloxacin on surface-modified carbon materials, Water Res., 45 (2011) 4583–4591.
[28] S. Carabineiro, T. Thavorn, M. Pereira, P. Serp, J. Figuiredo, Comparison between activated carbon, carbon xerogel and carbon nanotubes for the adsorption of the antibiotic ciprofloxacin, Catal. Today, 186 (2012) 29–34.
[29] A. Derylo-Marczewska, A. Swiatkowski, S. Biniak, M. Walczyk, Effect of properties of chemically modified activated carbon and aromatic adsorbate molecule on adsorption from liquid phase, Colloids Surf., A, 327 (2008) 1–8.
[30] V. Gómez-Serrano, F. Piriz, C.J. Duran-Valle, J. Pastor-Villegas, Formation of oxygen structures by air activation. A study by FT-IR spectroscopy, Carbon, 37 (1999) 1517–1528.
[31] A. Ip, J. Barford, G. McKay, Production and comparison of high surface area bamboo derived active carbons, Bioresour. Technol., 99 (2008) 8909–8916.
[32] F. Boudrahem, F. Aissani-Benissad, H. Ait-Amar, Batch sorption dynamics and equilibrium for the removal of lead ions from aqueous phase using activated carbon developed from coffee residue activated with zinc chloride, J. Environ. Manage., 90 (2009) 3031–3039.
[33] R.W. Coughlin, F.S. Ezra, Role of surface acidity in the adsorption of organic pollutants on the surface of carbon, Environ. Sci. Technol., 2 (1968) 291–297.
[34] A.C. de Oliveira Pimenta, J.E. Kilduff, Oxidative coupling and the irreversible adsorption of phenol by graphite, J. Colloid Interface Sci., 293 (2006) 278–289.
[35] D.D. Do, Adsorption Analysis: Equilibria and Kinetics: With CD Containing Computer Matlab Programs, World Scientific, Imperial College Press, London, 1998.